Proc. Natl. Acad. Sci. USA
Vol. 91, pp. 9412–9416, September 1994
Biochemistry

Toward solving the folding pathway of barnase: The complete backbone ^{13}C, ^{15}N, and ^{1}H NMR assignments of its pH-denatured state

(heteronuclear NMR/unfolded protein/folding)

VICKERY L. ARCUS, STEPHANE VUILLEUMIER†, STEFAN M. V. FREUND, MARK BYCROFT, AND ALAN R. FERSHT‡

Medical Research Council Unit for Protein Function and Design and Cambridge Centre for Protein Engineering, Department of Chemistry, University of Cambridge, Lensfield Road, Cambridge CB2 1EW, United Kingdom

Contributed by Alan R. Fersht, June 3, 1994

ABSTRACT **The structures of the major folding intermediate, the transition state for folding, and the folded state of barnase have been previously characterized. We now add a further step toward a complete picture of the folding of barnase by reporting the backbone ^{15}N, ^{13}C, and ^{1}H NMR assignments for barnase unfolded at pH 1.8 and 30°C. These assignments, which were obtained from a combination of heteronuclear magnetization transfer and backbone triple-resonance NMR experiments, constitute the first stage in the structural characterization of this denatured state by NMR. Interresidue nuclear Overhauser effect contacts and deviations from ^{1}H random-coil chemical shifts provide evidence for stable residual structure. The structured regions span residues in the native protein that contain its major α-helix and central strands of the β-sheet. Earlier experiments have shown that these regions are predominantly intact in the major folding intermediate and that their docking is partly rate determining in folding.**

Solving the pathway of folding of a protein requires detailed characterization of all the stable, metastable, and transition states adopted by the protein as it progresses from its unfolded state to its native structure. We have characterized in detail, by protein engineering methods and NMR, the major intermediate and transition state in the folding of barnase, a small extracellular ribonuclease (110 amino acids) from *Bacillus amyloliquefaciens* (1). We now need to determine the structures of states appearing earlier on the folding pathway. Conformations that occur very early are populated to a negligible extent under conditions favorable for folding and are thus inaccessible to techniques such as NMR. Under denaturing conditions, however, proteins may adopt conformations that are similar to those appearing early on the folding pathway. It follows that structural characterization of denatured states may provide insights into factors that govern early folding events (2, 3).

Determination of structure by NMR requires initially the assignment of all the resonances in a protein. The process of assignment is particularly difficult for denatured proteins because the dispersion of chemical shifts seen for native structures is largely lost on denaturation. There are two approaches to circumvent this problem, reviewed recently by Wüthrich (4). The first is to follow the transfer of heteronuclear magnetization, as reported by Wüthrich and colleagues for the 69-residue fragment of the phage 434 repressor (5, 6). By this approach, spectra are acquired for an equilibrium mixture of folded and unfolded states. The well-resolved resonances of the native state are correlated with those of the unfolded state via magnetization transfer. The second approach is to use multidimensional heteronuclear triple-resonance NMR experiments which have been developed for use with uniformly ^{15}N, ^{13}C-labeled proteins (7). Resonances are spread out in three dimensions according to their ^{1}H, ^{13}C, and ^{15}N chemical shifts, the latter retaining considerable dispersion even in the unfolded state. This procedure facilitates stepwise correlation of backbone ^{1}H, ^{15}N, and ^{13}C resonances and has very recently been applied to the assignment and structural characterization of the urea- and guanidinium chloride-denatured states of the FK506-binding protein (8).

Barnase has a cooperative and reversible unfolding transition between pH 2.8 and pH 2.0 at 30°C (M. Oliveberg, S.V., and A.R.F., unpublished results). Here we report the sequence-specific NMR assignment of barnase in the pH-denatured form, which constitutes the first major step in the characterization of this unfolded state by NMR. Magnetization transfer methods at the transition midpoint (pH = 2.4) provided sequence-specific assignments for 30% of the protein, and these assignments were confirmed and augmented, and the full assignment was completed by using three-dimensional (3D) backbone triple-resonance experiments.

MATERIALS AND METHODS

Barnase was purified from cultures of *Escherichia coli* (BL21) containing the plasmid pMT410 (9) as described previously (10, 11). Separate samples were produced of uniformly ^{15}N-labeled and uniformly ^{15}N, ^{13}C-labeled protein.

NMR samples at pH 2.9 and pH 1.8 were prepared by dissolving lyophilized protein in 0.5 ml of 90% H_2O/10% $^{2}H_2O$ (vol/vol) with appropriate concentrations of HCl. A sample at pH 2.4 additionally contained 50 mM glycine-d^5 buffer. The final concentrations for samples of uniformly ^{15}N-labeled barnase were 2.4 mM and for ^{15}N, ^{13}C-labeled barnase, 1.4 mM.

All NMR spectra were recorded at 30°C on a Bruker AMX500 spectrometer fitted with a fourth channel. Spectra were processed by using the Felix software package (Biosym Technologies, San Diego).

The ^{15}N and ^{1}H amide resonances for native barnase at pH 2.9 were assigned by reference to the full barnase assign-

The publication costs of this article were defrayed in part by page charge payment. This article must therefore be hereby marked "*advertisement*" in accordance with 18 U.S.C. §1734 solely to indicate this fact.

Abbreviations: 2D, two-dimensional; 3D, three-dimensional; COSY, correlation spectroscopy; TOCSY, total correlation spectroscopy; NOE, nuclear Overhauser effect; NOESY, NOE spectroscopy; HSQC, heteronuclear single quantum coherence; HMQC, heteronuclear multiple quantum coherence.

†Present address: Institut für Mikrobiologie, Eidgenössische Technische Hochschule, CH-8092 Zürich, Switzerland.
‡To whom reprint requests should be addressed.

ments at pH 4.5 (12) and a two-dimensional (2D) total correlation spectroscopy (TOCSY) ^{15}N–^{1}H heteronuclear multiple quantum coherence (HMQC) experiment (13) recorded at pH 2.9 with a mixing time of 55 ms. We acquired 4096 complex data points in t_2 with 256 t_1 increments and 160 scans per increment. These amide resonance assignments were then transferred to the pH-unfolded form by means of an exchange-relayed ^{15}N–^{1}H heteronuclear single quantum coherence (HSQC) spectrum (14) acquired at the transition midpoint (pH 2.4), using 4096 complex data points in t_2, 256 t_1 increments, 160 scans per increment, and a mixing time of 500 ms. This experiment yielded sequence-specific assignment for 33 residues in the pH-unfolded form. Concurrently, 103 amide ^{15}N, ^{1}H resonances were correlated with their $C^{\alpha}H$ and aliphatic side-chain spin systems by 2D and 3D ^{15}N–^{1}H TOCSY-HMQC spectra (13) acquired at pH 1.8 with, for the 3D TOCSY experiment, 512, 56, and 256 complex data points in t_3, t_2, and t_1 dimensions, respectively. Eight scans per increment were collected. In addition to the 33 residues sequence-specifically assigned (above), a further 46 spin systems could be unambiguously assigned to a residue type by reference to characteristic ^{1}H random-coil chemical shifts (15). Spectral overlap in 2D homonuclear spectra prevented the assignment of the ring protons of proline, phenylalanine, histidine, and tyrosine residues, with the exception of Tyr-17.

Given the above information as a template, the complete sequence-specific ^{15}N, ^{13}C, and ^{1}H backbone assignments were obtained by using three triple-resonance experiments: HNCA (16), HNCOCA (17) (see Fig. 2), and HNCACB (18). These correlate amide ^{15}N and ^{1}H resonances with adjacent $^{13}C^{\alpha}$ and, in the case of HNCACB, $^{13}C^{\beta}$ resonances. These spectra were acquired with uniformly ^{15}N, ^{13}C-labeled barnase at pH 1.8. In each case, the spectral width in the ^{1}H dimension was 6024 Hz and suppression of the water signal was achieved by presaturation and spin lock pulses (19). Quadrature detection was achieved in t_1 and t_2 by the States-TPPI method, and 16 scans per increment were collected. The HNCOCA and HNCACB experiments employed constant time evolution in the ^{15}N dimension (17) and in each case the spectral width in this dimension was 1572 Hz (see Fig. 2 for further acquisition and processing parameters). These three experiments gave assignments for all the backbone ^{1}H, ^{15}N, $^{13}C^{\alpha}$, and $^{13}C^{\beta}$ resonances.

Additional sequential information, from the observation of characteristic random-coil α, N (i, $i + 1$) connectivities, was given by a 3D ^{15}N–^{1}H nuclear Overhauser effect spectroscopy (NOESY) HMQC experiment (13) acquired with 512, 60, and 256 complex data points in t_3, t_2, and t_1 dimensions, respectively. A mixing time of 300 ms was used.

^{13}C carbonyl resonances were assigned by using the HNCO experiment (17), which correlates amide ^{15}N and ^{1}H resonances with the adjacent ^{13}C carbonyl (see Fig. 2 for acquisition and processing parameters).

Amide proton exchange rates for the pH-denatured form of barnase were measured at pH 2.0 and 30°C by dissolving lyophilized protein in $^{2}H_2O$ containing 0.03 M ^{2}HCl and following $^{1}H/^{2}H$ exchange with a series of ^{15}N–^{1}H HSQC spectra. Data for each amide were fitted to a single exponential to determine the rate constant for exchange, k_{ex}, and protection factors were calculated from the ratio k_{rc}/k_{ex}, where k_{rc} is the calculated intrinsic rate constant (20).

RESULTS

Fig. 1 shows the ^{15}N–^{1}H HSQC spectrum for barnase unfolded at pH 1.8 and 30°C. Sequence-specific assignments are shown for 106 residues—those missing are the N-terminal alanine and the three proline residues.

Initially, 33 sequence-specific assignments were obtained by following the exchange of ^{15}N–^{1}H heteronuclear magnetization (14) at the transition midpoint (pH = 2.4). This 2D ^{15}N–^{1}H correlation experiment allows the direct transfer of native assignments to the unfolded state. Two complete sets of peaks are seen in this spectrum, reflecting equal populations of the folded and unfolded states at pH 2.4. A third set of weaker peaks reflects the exchange of heteronuclear magnetization and relates the folded amide peaks with their unfolded counterparts. The intensity of these exchange peaks is dependent on the rate constant for unfolding/refolding and the mixing time used in this experiment (21). The unfolding rate constant for barnase at pH 2.4 is slow (0.1 s^{-1}) on this time scale and results in very weak exchange cross-peaks. In addition, the existence of three sets of peaks for each amide results in acute resonance overlap in the center of the spectral plane, and resolution of the folded peaks, unfolded peaks, and their symmetry-related cross-peaks is intractable in this region. Although this strategy could not provide a full amide ^{1}H, ^{15}N resonance assignment for pH-denatured barnase, it nevertheless gave crucial independent confirmation for assignments from subsequent triple-resonance experiments.

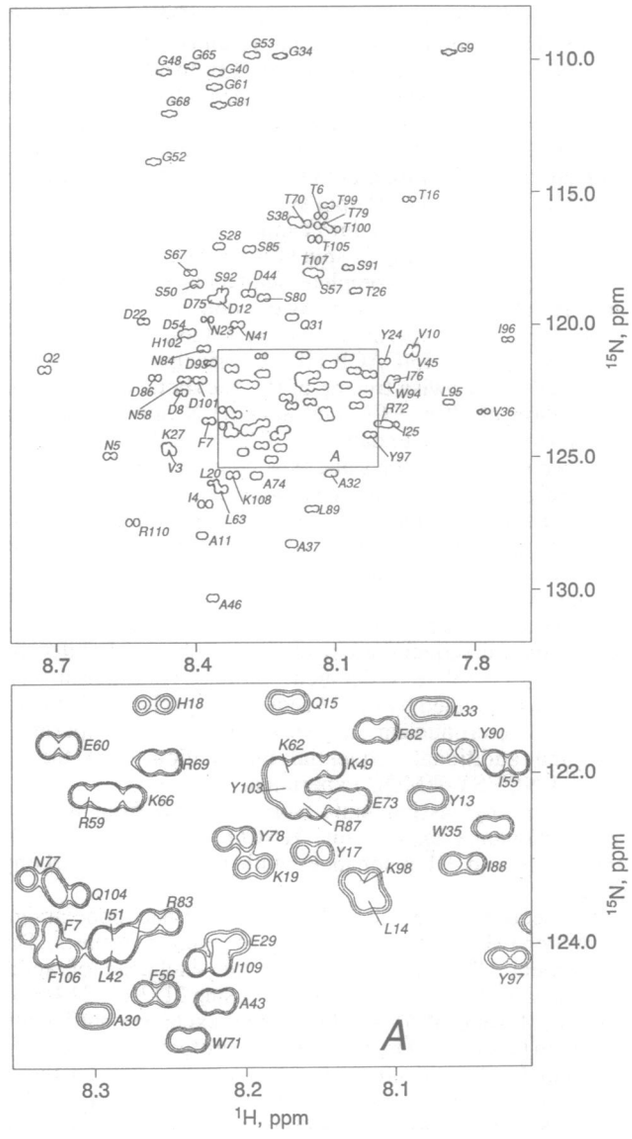

FIG. 1. The 2D ^{15}N–^{1}H HSQC spectrum of uniformly ^{15}N-labeled barnase in the pH-denatured state (2.4 mM protein concentration, 90% H_2O/10% $^{2}H_2O$ as a solvent, pH 1.8 and a temperature of 30°C). All backbone amides are assigned with the exception of Ala-1, which is not seen. Residues are in the one-letter code. Boxed area *A* in *Upper* is shown on an expanded scale in *Lower*.

The amide ^{1}H and ^{15}N resonances may be correlated with their $C^{\alpha}H$ and aliphatic side-chain ^{1}H spin systems by 2D and 3D ^{15}N–^{1}H TOCSY-HMQC spectra (13). In addition to the 33 residues sequence-specifically assigned (above) a further 46 spin systems could be unambiguously assigned to a residue type by the coincidence of their side-chain ^{1}H resonances with characteristic random-coil chemical shifts (15). Intraresidue NH, $C^{\alpha}H$, and $C^{\beta}H$ spin systems for aromatic, aspartic acid, and asparagine residues cannot be distinguished in this way, and the remaining 27 spin systems belong to this group.

Subsequently, the complete sequence-specific ^{15}N, ^{13}C, and ^{1}H backbone assignments were obtained by using three triple-resonance experiments: HNCA (16), HNCOCA (17) (see Fig. 2), and HNCACB (18). In principle, these experiments allow stepwise tracing of the backbone by sequential correlation of $^{13}C^{\alpha}$, $^{13}C^{\beta}$, and amide ^{15}N and ^{1}H chemical shifts. However, redundancy in $^{13}C^{\alpha}$ and $^{13}C^{\beta}$ chemical shifts between residues of the same type complicates this process. The assignment procedure can make use of this redundancy insofar as the $^{13}C^{\alpha}$ and $^{13}C^{\beta}$ chemical shifts uniquely identify residue types. Thus, sequential residue-type pairs are isolated and, where a sequence pair is unique for the protein, the sequence-specific assignment follows directly. It was the combination of identifying residue-type pairs in conjunction with standard sequential correlation of chemical shifts that led to the complete assignment. Crucial confirmatory evidence was provided by the 33 sequence-specific assignments from the heteronuclear magnetization transfer experiment (14) and additional sequential information from the 3D ^{15}N–^{1}H NOESY-HMQC experiment.

^{13}C carbonyl assignments were obtained from a fourth triple-resonance experiment, HNCO (17), correlating the amide ^{15}N and ^{1}H resonances with the adjacent carbonyl group.

The sequence-specific ^{15}N, ^{13}C, and ^{1}H backbone assignments for pH-denatured barnase are given in Table 1. This assignment allowed us to follow the exchange of amide protons with the solvent at pH 2.0, using 2D ^{15}N–^{1}H HSQC spectra. A total of 51 amide protons exchange sufficiently slowly to be followed by this method. Protection factors were calculated (20), and none were greater than 6.8. Of the 51 protection factors measured 47 lie within the range 0.7–3.5.

^{3}J HN–$C^{\alpha}H$ coupling constants were determined for 85 amide cross-peaks from an ^{15}N–^{1}H HSQC spectrum (J. Stonehouse and J. Keeler, personal communication). Coupling constants for residues of the same type are generally closely coincident. For example, values for the four glutamine residues in pH-denatured barnase range between 6.4 and 6.9 Hz. Similarly, values for the six asparagine residues range between 7.0 and 7.4 Hz. Comparatively small HN–$C^{\alpha}H$ couplings are seen, however, for Tyr-13, Leu-14, and Ala-30.

We have pursued a pluralistic approach to the NMR assignment of a denatured protein, combining both of the recently introduced methods. Backbone triple-resonance and heteronuclear magnetization transfer experiments provided independent sequence-specific assignments. Redundancy in the ^{1}H chemical shift data can also be utilized in the isolation of residue types from ^{1}H–^{15}N TOCSY experiments, and redundancy in ^{13}C chemical shifts facilitates the identification of sequential residue-type pairs from triple-resonance spectra.

DISCUSSION

Table 1 gives the complete sequence-specific ^{15}N, ^{13}C, and ^{1}H backbone assignments for pH-denatured barnase. Although these data will be used next for structural determination, they provide clues at this stage about the presence of stable residual structure. Some information may be inferred from resonances that show deviations from random-coil chemical shift values (underlined in Table 1). The great majority of proton chemical shifts lie within the characteristic ranges for random coil conformations; however, significant deviations are seen for the amide protons of Gly-9, Val-10, Val-36, Val-45, Leu-95, and Ile-96 (see Fig. 1) in conjunction with the side-chain protons of Thr-16, Val-36, Leu-95, and Ile-96. The majority of aromatic ^{1}H resonances, although not assigned,

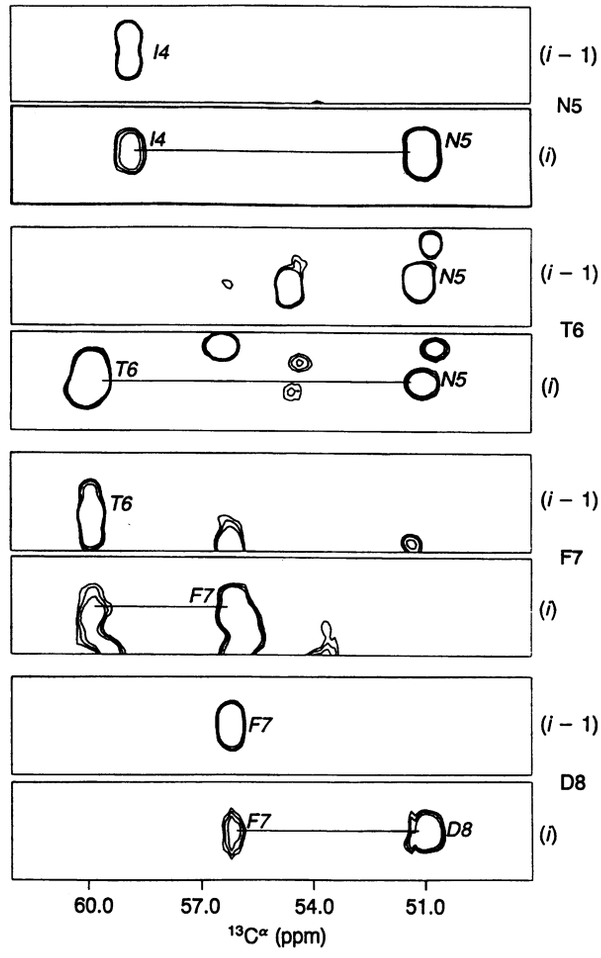

FIG. 2. Selected paired regions of the 3D HNCOCA and HNCA spectra acquired with uniformly ^{15}N, ^{13}C-labeled barnase in the pH-denatured state (1.4 mM protein, 90% H_2O/10% $^{2}H_2O$ as a solvent, pH 1.8, and 30°C) showing sequential connection of the $^{13}C^{\alpha}$ chemical shifts. The upper strip of each pair is taken from the HNCOCA spectrum. This correlates the amide ^{1}H and ^{15}N resonances of residue i with the $^{13}C^{\alpha}$ resonance of residue $i - 1$. The lower strip of each pair is taken from the HNCA spectrum correlating the amide ^{1}H and ^{15}N resonances of residue i with the $^{13}C^{\alpha}$ resonances of both residue i and residue $i - 1$. Sequential residue assignments are given to the right of each of the paired strips. Data for the HNCOCA experiment were acquired with a time-domain matrix of $32^{*}(t_1, {}^{15}N) \times 64^{*}(t_2, {}^{13}C) \times 512^{*}(t_3, {}^{1}H)$ data points, where n^{*} refers to n complex data points. Data for the HNCA experiment were acquired with a time-domain matrix of $42^{*}(t_1, {}^{15}N) \times 32^{*}(t_2, {}^{13}C) \times 512^{*}(t_3, {}^{1}H)$ data points and in both the HNCOCA and HNCA experiments the spectral width in the t_2, ^{13}C dimension was 3100 Hz. Data for the HNCACB experiment (not shown) were acquired with a time-domain matrix of $26^{*}(t_1, {}^{15}N) \times 128^{*}(t_2, {}^{13}C) \times 512^{*}(t_3, {}^{1}H)$ data points and here the t_2, ^{13}C spectral width was 7542 Hz. Finally, data for the HNCO experiment (not shown) were acquired with a time-domain matrix of $40^{*}(t_1, {}^{15}N) \times 32^{*}(t_2, {}^{13}C) \times 512^{*}(t_3, {}^{1}H)$ data points and a spectral width of 1250 Hz in the t_2, ^{13}C dimension. For all spectra, linear prediction of the last points was used to extend the time domain data in the t_1 (^{15}N) dimension, increasing the number of complex points by one-third. This was followed by shifted sine bell ($\pi/3$) apodization in all three dimensions and Fourier transformation. The real part of the 3D matrices contained 1024 × 256 × 128 data points.

Table 1. Backbone ^{15}N, ^{13}C, and ^{1}H chemical shifts* for pH-denatured barnase (pH = 1.8, 30°C)

Residue	^{15}N	C^{α}	C^{β}	C=O	NH	H^{α}	Residue	^{15}N	C^{α}	C^{β}	C=O	NH	H^{α}
A1		49.8	17.5	171.5			F56	124.55	55.8	37.6	173.6	8.25	4.75
Q2	121.77	53.9	27.9	173.5	8.72	4.51	S57	118.06	56.5	61.9	172.3	8.13	4.48
V3	124.77	60.6	31.0	173.9	8.45	4.21	N58	122.13	51.0	36.7	173.4	8.42	4.78
I4	126.77	58.9	37.0	173.7	8.37	4.28	R59	122.30	54.5	28.7	174.4	8.30	4.39
N5	125.00	51.1	37.2	173.2	8.57	4.86	E60	121.69	54.0	26.9	174.4	8.32	4.42
T6	115.91	60.1	68.1	172.3	8.12	4.38	G61	111.03	43.3		172.1	8.35	4.04, 4.00
F7	123.66	56.2	37.5	173.6	8.37	4.67	K62	121.96	54.1	31.4	174.3	8.17	4.34
D8	122.48	51.0	36.1	173.3	8.43	4.71	L63	126.29	54.2	40.0	†	8.34	4.70
G9	109.77	43.6		172.2	7.86	3.97	P64		61.4	30.1	175.5		
V10	120.86	60.9	31.0	174.1	7.93	4.12	G65	110.27	43.2		172.2	8.40	4.08, 4.00
A11	127.94	51.1	17.1	175.8	8.37	4.32	K66	122.26	54.4	31.3	174.9	8.28	4.43
D12	119.12	51.4	36.1	173.4	8.34	4.70	S67	118.06	56.7	62.0	173.0	8.40	4.57
Y13	122.34	57.1	36.7	174.1	8.07	4.52	G68	112.08	43.4		172.1	8.45	4.10, 4.05
L14	123.55	53.9	40.4	175.7	8.11	4.31	R69	121.88	54.4	29.1	174.6	8.25	4.44
Q15	121.15	54.6	27.4	174.2	8.17	4.35	T70	116.21	60.1	68.1	172.3	8.16	4.44
T16	115.25	60.7	68.0	172.3	7.93	4.24	W71	125.19	55.7	27.8	173.9	8.23	4.73
Y17	122.88	56.4	36.9	173.5	8.14	4.54	R72	123.80	54.2	29.1	173.9	8.00	4.24
H18	121.14	53.2	26.9	171.4	8.26	4.65	E73	122.37	54.0	26.9	173.7	8.13	4.28
K19	123.02	54.2	31.5	173.8	8.18	4.36	A74	125.72	50.7	17.5	175.4	8.26	4.34
L20	126.00	51.0		†	8.35	4.65	D75	119.03	51.2	36.1	173.0	8.35	4.75
P21		61.1	30.0	174.7			I76	122.04	59.4	37.0	173.5	7.97	4.17
D22	119.89	51.3	36.0	172.9	8.50	4.67	N77	123.26	51.0	37.1	172.9	8.33	4.77
N23	119.73	51.2	36.7	172.6	8.38	4.72	Y78	122.84	56.5	37.0	174.2	8.20	4.66
Y24	121.45	56.4	36.8	173.5	7.99	4.74	T79	116.29	60.1	68.2	172.6	8.12	4.42
I25	123.76	59.2	36.9	174.1	7.97	4.27	S80	119.06	56.9	62.0	173.0	8.25	4.49
T26	118.71	59.8	68.2	172.9	8.04	4.40	G81	111.74	43.3		171.9	8.34	4.01, 3.97
K27	124.55	55.8	31.0	175.4	8.46	4.33	F82	121.57	56.1	37.7	173.9	8.10	4.65
S28	117.02	57.4	61.5	173.6	8.34	4.45	R83	123.71	54.2	28.9	173.9	8.25	4.32
E29	124.03	54.8	26.7	174.5	8.21	4.34	N84	120.95	51.8	37.0	173.4	8.38	4.73
A30	124.73	51.7	16.9	176.6	8.30	4.18	S85	117.18	56.9	61.9	172.4	8.28	4.48
Q31	119.69	54.9	27.3	174.7	8.20	4.29	D86	122.08	51.3	36.0	171.9	8.48	4.77
A32	125.63	51.2	17.0	176.2	8.09	4.31	R87	122.37	54.5	28.8	174.1	8.16	4.34
L33	121.19	53.6	40.5	176.1	8.06	4.33	I88	123.02	59.4	36.6	173.9	8.05	4.14
G34	109.82	43.6		172.2	8.22	4.01	L89	127.00	53.2	40.6	174.8	8.14	4.35
W35	122.69	55.8	27.7	174.2	8.03	4.71	Y90	121.70	56.0	37.0	173.9	8.05	4.63
V36	123.18	60.2	31.4	173.4	7.78	4.02	S91	117.87	56.5	62.0	172.7	8.06	4.42
A37	128.33	50.8	17.3	175.9	8.19	4.22	S92	118.82	57.1	61.8	172.6	8.34	4.44
S38	116.10	56.5	62.0	172.7	8.18	4.47	D93	121.48	51.5	35.9	173.1	8.36	4.64
K39	124.10	54.8	31.0	175.1	8.33	4.39	W94	122.32	56.1	27.4	174.2	7.98	4.67
G40	110.49	43.4		171.8	8.35	4.00	L95	122.99	54.0	40.3	175.4	7.85	4.21
N41	120.06	51.3	37.0	173.4	8.31	4.79	I96	120.56	59.8	36.7	174.3	7.73	4.09
L42	124.05	53.5	40.3	175.2	8.28	4.33	Y97	124.18	56.2	36.8	173.8	8.02	4.63
A43	124.71	50.8	17.3	175.5	8.21	4.36	K98	123.28	54.7	31.2	174.6	8.12	4.36
D44	118.81	51.0	36.2	172.8	8.28	4.79	T99	115.53	60.2	68.0	172.8	8.11	4.46
V45	121.07	60.1	31.1	173.3	7.94	4.21	T100	116.41	60.2	68.0	172.2	8.10	4.42
A46	130.33	48.5	16.4	†	8.35	4.66	D101	122.15	51.0	36.1	172.7	8.38	4.80
P47		61.4	30.1	175.7			H102	120.35	53.4	26.8	172.9	8.42	4.70
G48	110.49	43.3		171.7	8.46	4.03	Y103	122.13	56.1	36.9	173.5	8.16	4.70
K49	121.99	54.2	31.4	174.6	8.15	4.41	Q104	123.43	53.8	28.0	173.5	8.32	4.42
S50	118.54	56.2	62.0	172.6	8.39	4.59	T105	116.78	59.8	68.1	172.1	8.14	4.36
I51	123.94	59.6	37.0	174.7	8.29	4.34	F106	123.84	55.9	37.9	173.9	8.33	4.80
G52	113.91	43.4		172.5	8.48	4.07, 4.03	T107	118.01	60.0	68.2	171.8	8.15	4.37
G53	109.80	43.2		172.0	8.27	4.03	K108	125.72	54.4	31.2	174.1	8.31	4.40
D54	120.25	50.8	36.2	173.1	8.41	4.79	I109	124.21	59.3	36.9	174.1	8.22	4.24
I55	121.86	59.7	36.6	174.0	8.03	4.18	R110	127.62	53.3	28.5		8.53	4.43

*Proton chemical shift values are relative to internal 3-trimethylsilylpropanoic-d_4 acid. ^{1}H chemical shifts are underlined if they deviate from random coil values by more than 0.1 ppm for nonlabile protons and 0.3 ppm for amide protons. ^{15}N chemical shift values are relative to external ^{15}N-substituted ammonium chloride, and ^{13}C chemical shifts are indirectly referenced to the solvent ^{1}H frequency (22). Side-chain proton assignments are not shown; however, these are complete except for the ring protons of proline, phenylalanine, histidine, and tyrosine, which could not be assigned due to spectral overlap. Assignments for the aromatic protons of Tyr-17 and the three tryptophan residues have been determined.

†^{13}C carbonyl chemical shifts cannot be determined for the three residues preceding proline.

are also in close agreement with random-coil values, with the exception of the $C^{\delta}H$ of Tyr-17, which deviates from random coil by 0.1 ppm. Deviations from random-coil values for ^{13}C resonances (23) are quite uniform along the length of the protein and do not provide complementary information.

The weak evidence for stable residual structure from the deviations in chemical shift is considerably strengthened by the observation of a number of interresidue NOE peaks that are inconsistent with extended-strand conformations. These include strong sequential H^N–H^N (i, $i + 1$) NOE contacts for residues Asp-93–Tyr-97, Asp-12–Tyr-13, and Thr-16–Tyr-17 and a number of aromatic to methyl NOE contacts whose assignments are tentative. It must be noted that no other strong H^N–H^N (i, $i + 1$) NOE contacts are observed across the protein, and those for Asp-93–Tyr-97 are nonnative, while those for Asp-12–Tyr-13 and for Thr-16–Tyr-17 are native-like (the major helix in barnase extends from Thr-6 to His-18). The small ^{3}J HN–$C^{\alpha}H$ coupling constants seen for Tyr-13 and Leu-14 provide further evidence that residual structure persists in this region. Heteronuclear edited NOE experiments should allow us to characterize the structure of pH-denatured barnase in detail.

The protection of amide protons against exchange with solvent is generally used as evidence that these groups are involved in hydrogen bonding or structured interactions. We do not see significantly large protection factors for pH-denatured barnase. It is important to note, however, that for structured conformations in fast exchange with unstructured conformations, small protection factors may represent, in reality, very significant interactions of amides. This is be-

cause exchange occurs rapidly from the unstructured state, which masks the protection in the structured state. If we assume a rapid equilibrium between structured and unstructured states and, further, that a particular amide has significant protection in a structured state whose population in solution is, say, 75%, then the upper limit for its protection factor is just 4.0. It follows that the presence of structured regions is not inconsistent with the small protection factors observed for pH-denatured barnase, provided the structured states are in fast exchange with unstructured states.

Chemical shift, NOE, and coupling constant data thus provide compelling evidence for the presence of small areas of stable residual structure in the pH-denatured form of barnase and in particular the regions encompassing Gly-9–Tyr-17 and Asp-93–Tyr-97. The importance of these observations is that it is precisely these regions that have been implicated from the earlier protein engineering experiments to be formed early in protein folding and whose docking is partly rate determining (1). Detailed characterization of these stable structured conformations is now possible, given the full NMR assignment reported here, and this will provide the basis for analysis of the initial events in protein folding.

We thank the members of the Wüthrich laboratory in general and Dr. Dario Neri and Dr. Gerhard Wider in particular for their help in the implementation of the magnetization transfer experiments.

1. Fersht, A. R. (1993) *FEBS Lett.* **325**, 5–16.
2. Shortle, D. (1993) *Curr. Opin. Struct. Biol.* **3**, 66–74.
3. Dobson, C. M. (1992) *Curr. Opin. Struct. Biol.* **2**, 6–12.
4. Wüthrich, K. (1994) *Curr. Opin. Struct. Biol.* **4**, 93–99.
5. Neri, D., Billeter, M., Wider, G. & Wüthrich, K. (1992) *Science* **257**, 1559–1563.
6. Neri, D., Wider, G. & Wüthrich, K. (1992) *Proc. Natl. Acad. Sci. USA* **89**, 4397–4401.
7. Kay, L. E., Ikura, M., Tschudin, R. & Bax, A. (1990) *J. Magn. Reson.* **89**, 496–514.
8. Logan, T. M., Thériault, Y. & Fesik, S. W. (1994) *J. Mol. Biol.* **236**, 637–648.
9. Paddon, C. J. & Hartley, R. W. (1987) *Gene* **53**, 11–19.
10. Mossakowska, D. E., Nyberg, K. & Fersht, A. R. (1989) *Biochemistry* **28**, 3843–3850.
11. Jones, D. N. M., Bycroft, M., Lubienski, M. J. & Fersht, A. R. (1993) *FEBS Lett.* **331**, 165–172.
12. Bycroft, M., Sheppard, R. N., Lau, F. T.-K. & Fersht, A. R. (1990) *Biochemistry* **29**, 7425–7432.
13. Marion, D., Driscoll, P. C., Kay, L. E., Wingfield, P. T., Bax, A., Gronenborn, A. M. & Clore, G. M. (1989) *Biochemistry* **28**, 6150–6156.
14. Wider, G., Neri, D. & Wuthrich, K. (1991) *J. Biomol. NMR* **1**, 93–98.
15. Wüthrich, K. (1986) *NMR of Proteins and Nucleic Acids* (Wiley, New York).
16. Farmer, B. T., II, Venters, R. A., Spicer, L. D., Wittekind, M. G. & Müller, L. (1992) *J. Biomol. NMR* **2**, 195–202.
17. Grzesiek, S. & Bax, A. (1992) *J. Magn. Reson.* **96**, 432–440.
18. Wittekind, M. & Mueller, L. (1993) *J. Magn. Reson. Ser. B* **101**, 201–205.
19. Messerle, B. A., Wider, G., Otting, G., Weber, C. & Wüthrich, K. (1989) *J. Magn. Reson.* **85**, 608–613.
20. Bai, Y., Milne, J. S., Mayne, L. & Englander, S. W. (1993) *Proteins* **17**, 75–86.
21. Ernst, R. R., Bodenhausen, G. & Wokaun, A. (1987) *Principles of Nuclear Magnetic Resonance in One and Two Dimensions* (Clarendon, Oxford).
22. Bax, A. & Subramanian, S. (1986) *J. Magn. Reson.* **67**, 565–569.
23. Howarth, W. O. & Lilley, D. M. (1978) *Progress NMR Spectroscopy* **12**, 1–40.